Characterization of Vibrational Resonances of Water-Vapor Interfaces by Phase-Sensitive Sum-Frequency Spectroscopy

N. Ji,[*] V. Ostroverkhov,[†] C. S. Tian, and Y. R. Shen[‡]

Department of Physics, University of California, and Materials Sciences Division, Lawrence Berkeley National Laboratory, Berkeley, California 94720, USA

Phase-sensitive sum-frequency spectroscopy provides correct characterization of vibrational resonances of water-vapor interfaces and allows better identification of interfacial water species contributing to different parts of the spectra. Iodine ions emerging at an interface create a surface field that tends to reorient the more loosely bonded water molecules below the topmost layer.

Understanding how water interfaces play key roles in many relevant physical, chemical, and biological processes requires knowledge of water interfacial structures at the molecular level [1]. Orientations and bonding arrangement of water molecules at an interface affect the interface properties and hence the interfacial processes. Vapor-water interfaces, in particular, have attracted much recent interest not only because they are important in environmental science, but also because they serve as standard references for water interfaces. Surface-specific sum-frequency vibrational spectroscopy (SFVS) has been applied extensively to the interfaces. Early results show the appearance of a dangling OH stretch mode and the appearance of liquid-like and ice-like features in the spectrum, indicating that the water surface is a disordered hydrogen (H)-bonding network terminated by broken bonds on H and O of topmost water molecules [2,3]. More recently, studies have focused on which water species at the interfaces contribute to which part of the spectrum, and how ions may emerge at the surface to alter the interfacial structure and change the spectrum [3–11].

The SF vibrational spectra of water interfaces reported so far are all intensity spectra proportional to $|\chi_S^{(2)}(\omega_{SF} = \omega_{vis} + \omega_{IR})|^2$ with $\chi_S^{(2)}$ being the surface nonlinear susceptibility [12]. Because the interfacial water molecules experience wide variation of H-bonding geometries and strengths, the spectra appear as continuous, highly inhomogeneously broadened bands [13]. Analysis to decompose a spectrum into a set of discrete resonances is generally not unique, and has led to a great deal of confusion in the literature [3–11]. It is clear that in order to characterize the resonances, one needs to know $Im\chi_S^{(2)}$ in analogy to $Im\varepsilon$ in linear spectroscopy, or more completely, both $Re\chi_S^{(2)}$ and $Im\chi_S^{(2)}$. For a band of resonances, it is not possible to deduce $Im\chi_S^{(2)}$ from $|\chi_S^{(2)}|^2$. We must obtain $Im\chi_S^{(2)}$ directly from measurement. We report here the first vibrational spectra of $Im\chi_S^{(2)}$ for water-vapor interfaces of pure water and NaI solution acquired by a phase-sensitive(PS)-SFVS technique. They are clearly different from those obtained from analyses of $|\chi_S^{(2)}|^2$ with assump-

tion of discrete resonances. The results facilitate our identification of various interfacial water species contributing to the different parts of the spectra.

The PS-SFVS technique was described elsewhere [14,15]. Briefly, we interfered the SF signal from the water-vapor interface with that from a reference crystal over the spectral range of interest and then deduced from the measurement both the amplitude and the phase of $\chi_S^{(2)}$, and hence $Re\chi_S^{(2)}$ and $Im\chi_S^{(2)}$. The spectra of $Re\chi_S^{(2)}$, $Im\chi_S^{(2)}$, and $|\chi_S^{(2)}|^2$ of a pure water-vapor interface ($pH \sim 5.7$) in the OH stretch range are displayed in Fig. 1. We focus here on $Im\chi_S^{(2)}$ because it is most informative. As seen in the figure, $Im\chi_S^{(2)}$ roughly consists of three bands, a positive peak at ~ 3700 cm^{-1}, a negative band from ~ 3200 to 3600 cm^{-1}, and a positive band below 3200 cm^{-1}. They correspond to features in the $|\chi_S^{(2)}|^2$ spectrum previously labeled as dangling OH, liquid-like, and ice-like peaks, respectively [16]. Our $Im\chi_S^{(2)}$ spectrum differs significantly from those deduced from fitting of the
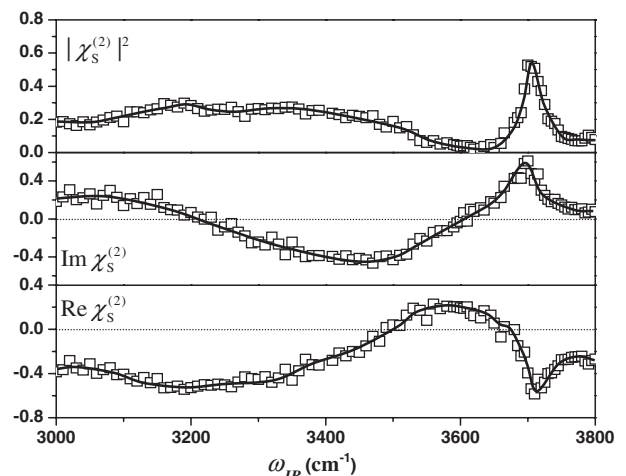

FIG. 1. Spectra of $|\chi_S^{(2)}|^2$, $Im\chi_S^{(2)}$, and $Re\chi_S^{(2)}$ for neat water-vapor interface in the OH stretch range obtained with the phase-sensitive sum-frequency vibrational spectroscopy (PS-SFVS). The curves are for eye guiding.

$|\chi_S^{(2)}|^2$ spectrum with discrete resonances [6–11,17] and MD simulations [18–20]. A series of recent papers, for example, concluded from fitting that both ice-like and liquid-like bands are opposite in sign with respect to the dangling OH peak, in disagreement with our result. As mentioned earlier, fitting a highly inhomogeneously broadened $|\chi_S^{(2)}|^2$ spectrum with discrete resonances is generally not appropriate. MD simulations are also limited by compromises used in the calculations. The spectra calculated by Morita and Haynes agreed qualitatively with ours above 3200 cm^{-1}, but there are difficulties for theory to relate interfacial water species with spectral features [21]. Our direct measurement of the Im$\chi_S^{(2)}$ spectrum now permits more reliable spectral assignment to water species and structure at the water-vapor interface.

In interpreting the Im$\chi_S^{(2)}$ spectrum, we consider the surface structure of water as a heavily distorted H-bonding network of the hexagonal ice surface [Fig. 2(a)]. Interfacial molecules are H-bonded to neighbors with a continuous variation of (or dynamically varying) geometries and strengths. D and A label donor and acceptor H-bonds, respectively, through which a water molecule connects to neighbors. A donor bond, directly affecting the electron distribution around H, causes the OH stretch frequencies to shift much more than an acceptor bond [22]. The topmost surface layer is mainly occupied by DAA and DDA molecules [3]. DAA has a dangling OH pointing towards the vapor side, and DDA has its oxygen facing the vapor. The surface-specific SF vibrational spectrum originates essentially from DAA and DDA molecules of the topmost layer and $DDAA$ molecules of the adjacent layers; the subsequent layers have little contribution because the surface structure rapidly relaxes to that of the bulk. With these considerations, we can relate the spectral features to the water interfacial structure consistently.

The positive sharp band above 3600 cm^{-1} in the Im$\chi_S^{(2)}$ spectrum can be attributed to OH stretches of the DAA molecules. The free and donor-bonded OHs of DAA are coupled in general to yield symmetric (s-) and antisymmetric (a-) stretch modes. However, if the donor bond is sufficiently strong, the two modes are essentially decoupled with their transition dipole moments along the two OH bonds, respectively. (For numerical estimates, see description in Ref. [23].) It is then clear that the original a-stretch has the dipole moment along the dangling free OH and is responsible for the positive peak at $\sim$3700 cm^{-1}. The original s-stretch has the dipole moment along the donor-bonded OH pointing toward the liquid bulk and contributes to the negative band below 3600 cm^{-1} in the Im$\chi_S^{(2)}$ spectrum. There appears a weak but broad positive hump around the sharp peak in the Im$\chi_S^{(2)}$ spectrum, which possibly comes from DAA molecules with a weak donor bond. In this case, coupling between the two OHs is no longer negligible, and the s-mode could appear above 3600 cm^{-1} and its transition
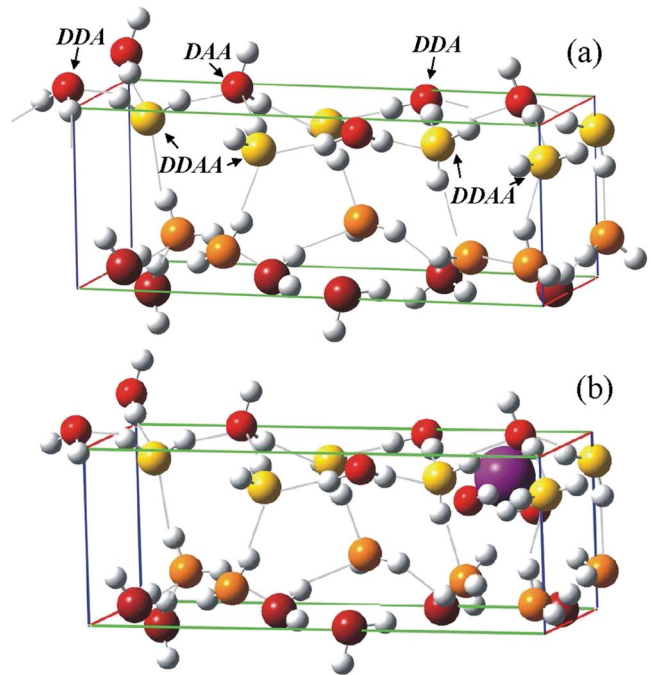

FIG. 2 (color). Cartoons describing the structures of water-vapor interfaces of (a) neat water and (b) NaI solution. The interfacial water structure is modeled after a distorted hexagonal ice. The top layer of the topmost layer (oxygen marked red) is occupied by DAA and DDA molecules, and the second layer (oxygen marked yellow) is occupied by $DDAA$ molecules. Some $DDAA$ molecules connecting to the molecules in the top layer with two donor bonds have an overall ice-like tetrahedral bonding structure. They contribute to the ice-like part of the vibrational spectrum. Other $DDAA$ molecules are less symmetrically bonded to neighbors and contribute to the spectrum in the higher frequency region. The third and fourth layers (marked orange and red, respectively) have molecules with increasing randomness in position and orientation, closely resembling that of liquid water. In (b), an iodine ion straddled by water molecules at the lower side is shown to appear near the surface. It disrupts mainly the nearby water bonding structure beneath the topmost monolayer and reorients the more loosely bonded subphase molecules by the field it has created.

dipole moment pointing toward the vapor side. The corresponding a-mode would appear slightly above 3720 cm^{-1}. This assignment is supported by the observation that both the sharp peak and the broad base disappear when the dangling OH is terminated, as in the case of water-quartz interface [14].

The negative band between 3200 and 3600 cm^{-1} in the Im$\chi_S^{(2)}$ spectrum resembles the absorption band of bulk liquid water, although different in signs. As in bulk water, it comes mainly from OH of asymmetrically H-bonded water molecules of varying strengths and geometries. They must be the donor-bonded OH of DAA and DDA molecules in the topmost layer at the interface and the asymmetrically donor-bonded $DDAA$ in the adjacent layers [2,3]. The first two clearly have their stretch dipole moments pointing toward liquid. The asymmetrically

donor-bonded *DDAA* molecules beneath the topmost layer also have an average stretch dipole moment point toward the liquid. This can be seen as follows. If all subsurface *DDAA* molecules were asymmetrically bonded with equal probability in configurations having dipoles pointing up and down, the net polar orientation would be zero. However, the interfacial *DDAA* molecules that straddle the oxygen atoms of *DAA* and *DDA* in the topmost layer, with both donor bonds pointing toward vapor, are partly symmetrically bonded (contributing to the ice-like band as will be discussed later) and partly asymmetrically donor-bonded. Only the asymmetrically donor-bonded *DDAA* molecules contribute to the liquid-like band. Their total upward dipole moment is now overwhelmed by the total downward dipole moment of the other asymmetrically bonded *DDAA* molecules at the interface, resulting in an overall negative contribution to the liquid-like band. The wide variation of the H-bonding strength in the above-mentioned water species leads to the wide range of OH stretch frequencies, and hence the broad liquid-like band. It is known that annealing of amorphous ice reduces the IR absorption in the 3300–3600 cm^{-1} region and increases in the 3000–3200 cm^{-1} region [24]. This supports the assignment that the liquid-like band comes from OHs not orderly bonded to neighbors. As we shall discuss later, study of the water-vapor interface of a NaI solution allows us to further identify *DAA* and *DDA* as major contributors to the higher-frequency part and *DDAA* to the lower-frequency part of the liquid-like band.

Finally, the positive band below 3200 cm^{-1} is the ice-like band. It comes from *DDAA* molecules with ice-like symmetric tetrahedral bonding to neighbors. The main contribution is from those *DDAA* molecules that straddle *DDA* and *DAA* molecules in the topmost layer with symmetric donor bonds. The *s*-stretch modes of these molecules have their stretch dipole moment point towards the vapor side and hence contribute positively to the band. The corresponding *a*-stretch has a dipole moment incline towards the surface and contributes much less. Because of the rapidly decreasing order of H-bonding in the transition layers toward the bulk, there are considerably fewer *DDAA* molecules in other symmetric bonding geometry, such as those with only one H donor-bonded to *DAA* or *DDA*, and their contributions are much less important. The ice-like and liquid-like bands overlap around 3200 cm^{-1}, resulting in the crossover from positive to negative around 3200 cm^{-1} in the Im$\chi_S^{(2)}$ spectrum.

Recently, the question whether solvated ions come to the water-vapor interface and alter the water interfacial structure and properties has attracted much attention. Contrary to earlier prediction, MD simulations suggested that large negative ions could appear at the interface [25]. Indeed, SFVS studies showed a significant enhancement of the liquid-like band and the appearance of a broad shoulder above the 3700 cm^{-1} peak in the $|\chi_S^{(2)}|^2$ spectrum when 0.036*x* NaI was added into bulk water [6,11]. By fitting the

spectrum, one group attributed the changes to I^- ions disrupting the interfacial H-bonding network and creating more asymmetrically H-bonded molecules as well as increasing the effective interfacial layer thickness [6]. Another group concluded that there was no significant changes in the mode strengths of H-bonded OH, and the change of the spectrum was due to blueshift and narrowing of the mode at ~3400 cm^{-1} [11]. The contradicting interpretations result from different fittings of $|\chi_S^{(2)}|^2$, which can be avoided if the Im$\chi_S^{(2)}$ spectrum is directly measured.

Figure 3 displays the spectra of $|\chi_S^{(2)}|^2$, Re$\chi_S^{(2)}$, and Im$\chi_S^{(2)}$, for the vapor/liquid interface of a 0.036*x* NaI solution. For comparison, we also sketch in Fig. 3 the corresponding spectra for the neat water-vapor interface. Our $|\chi_S^{(2)}|^2$ spectrum (before removing the Fresnel coefficients) for the NaI solution shows good agreement with others. The Im$\chi_S^{(2)}$ spectrum is more informative. Compared with the case of neat water, the obvious changes are expansion of the positive ice-like band to 3350 cm^{-1}, shrinkage of the negative liquid-like band, and appearance of a broad positive shoulder on the high-frequency side of the dangling OH peak. There are no significant changes below 3100 cm^{-1} and between 3450 and 3720 cm^{-1}. In Fig. 3, we also show the Im$\chi_S^{(2)}$ spectrum for a 0.019*x* NaI solution. It exhibits the same behavior except for the extension of the positive ice-like band to only 3300 cm^{-1}. Our spectra qualitatively resemble those predicted by recent MD simulations [20].

The I^- ions at the water-vapor interface may disturb the interfacial H-bonding structure as well as create a surface field that reorients part of the interfacial water molecules toward the vapor side. Since only a small number of I^- ions would be present in the topmost layer [26,27], their
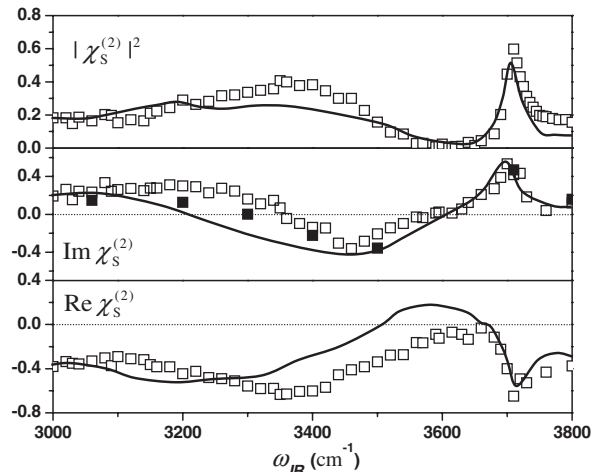

FIG. 3. Spectra of $|\chi_S^{(2)}|^2$, Im$\chi_S^{(2)}$, and Re$\chi_S^{(2)}$ for water-vapor interface of a 0.036*x* NaI solution in the OH stretch range. For comparison, the eye-guiding spectra for the neat water-vapor interface from Fig. 1 are displayed. Solid squares in Im$\chi_S^{(2)}$ are data points at discrete frequencies on the Im spectrum for the water-vapor interface of a 0.019*x* NaI solution.

disturbance on the bonding structure of molecules in the topmost layer is small, and the major effect of the I^- ions at the interface is on the more loosely asymmetrically bonded *DDAA* molecules connected to the topmost layer. Such *DDAA* molecules are more easily reoriented by the ion-created surface field to have their dipoles pointing more towards the vapor side. The lack of significant changes in the spectral feature from 3420 to 3710 cm^{-1} and the ice-like feature below 3100 cm^{-1} therefore suggests that the former come from donor-bonded OH of *DAA* and *DDA* molecules in the topmost layer and the latter from *DDAA* molecules with stronger symmetric donor bonds straddling *DAA* and *DDA* in the topmost layer. The observed spectral change in the 3200–3400 cm^{-1} region indicates that it is OH stretches of the asymmetrically bonded *DDAA* molecules that contribute significantly to this spectral region, and the field-induced reorientation of such molecules makes Im$\chi_S^{(2)}$ more positive in this region. The interfacial I^- ions also induce a positive shoulder above 3720 cm^{-1}. It likely comes from water molecules straddling the interfacial ions, mostly from the bottom side of the ions due to paucity of water molecules on the vapor side. Weaker bonding to I^- ions, and perhaps also their weaker acceptor bonding to other water molecules due to geometric distortion, blueshift their OH stretch frequencies. A cartoon for the interfacial water structure with the presence of I^- is shown in Fig. 2(b).

The work here shows that the spectrum of Im$\chi_S^{(2)}$ obtained with PS-SFVS can provide a much clearer picture of water-vapor interfacial structure. While the overall broad spectrum comes from inhomogeneous broadening of OH stretches with continuous variation of H-bonding geometry and strength, molecular species contributing to different spectral ranges can be reasonably identified. Hydrated ions appearing at the interface may not disturb significantly the molecular bonding structure in the topmost surface layer, but the surface field they create could partially reorient molecules in the subphase. These could be general rules for water-vapor interfaces of salt, acid, and base solutions, and will be tested in future studies. Likewise, spectroscopic measurements of Im$\chi_S^{(2)}$ are expected to yield better structural information on other water interfaces.

---

*Present address: Janelia Farm Research Campus, Howard Hughes Medical Institute, Ashburn, VA 20147, USA

†Present address: General Electric Global Research, Niskayuna, NY 12309, USA

‡To whom correspondence should be addressed: yrshen@calmail.berkeley.edu

[1] P. Jungwirth, Chem. Rev. **106**, 1137 (2006).

[2] Q. Du, E. Freysz, and Y. R. Shen, Science **264**, 826 (1994).

[3] Q. Du, R. Superfine, E. Freysz, and Y. R. Shen, Phys. Rev. Lett. **70**, 2313 (1993).

[4] D. E. Gragson, B. M. McCarty, and G. L. Richmond, J. Phys. Chem. **100**, 14272 (1996).

[5] S. Baldelli, C. Schnitzer, M. J. Shultz, and D. J. Campbell, J. Phys. Chem. B **101**, 10435 (1997).

[6] D. Liu, G. Ma, L. M. Levering, and H. C. Allen, J. Phys. Chem. B **108**, 2252 (2004).

[7] W. Gan, D. Wu, Z. Zhang, R. Feng, and H. Wang, J. Chem. Phys. **124**, 114705 (2006).

[8] X. Wei, P. B. Miranda, and Y. R. Shen, Phys. Rev. Lett. **86**, 1554 (2001).

[9] M. G. Brown, E. A. Raymond, H. C. Allen, L. F. Scatena, and G. L. Richmond, J. Phys. Chem. A **104**, 10220 (2000).

[10] E. A. Raymond, T. L. Tarbuck, and G. L. Richmond, J. Phys. Chem. B **106**, 2817 (2002).

[11] E. A. Raymond and G. L. Richmond, J. Phys. Chem. B **108**, 5051 (2004).

[12] Y. R. Shen, in *Proceedings of the International School of Physics "Enrico Fermi"*, Course CXX, Frontiers in Laser Spectroscopy (North Holland, Amsterdam, 1994).

[13] P. B. Petersen and R. J. Saykally, Annu. Rev. Phys. Chem. **57**, 333 (2006).

[14] V. Ostroverkhov, G. A. Waychunas, and Y. R. Shen, Phys. Rev. Lett. **94**, 046102 (2005).

[15] N. Ji, V. Ostroverkhov, C.-Y. Chen, and Y. R. Shen, J. Am. Chem. Soc. **129**, 10056 (2007).

[16] Y. R. Shen and V. Ostroverkhov, Chem. Rev. **106**, 1140 (2006).

[17] S. Gopalakrishnan, P. Jungwirth, D. J. Tobias, and H. C. Allen, J. Phys. Chem. B **109**, 8861 (2005).

[18] A. Perry *et al.*, J. Chem. Phys. **123**, 144705 (2005).

[19] E. C. Brown, M. Mucha, P. Jungwirth, and D. J. Tobias, J. Phys. Chem. B **109**, 7934 (2005).

[20] T. Ishiyama and A. Morita, Chem. Phys. Lett. **431**, 78 (2006).

[21] A. Morita and J. T. Hynes, J. Phys. Chem. B **106**, 673 (2002).

[22] H. M. Lee, S. B. Suh, J. Y. Lee, P. Tarakeshwar, and K. S. Kim, J. Chem. Phys. **112**, 9759 (2000).

[23] See EPAPS Document No. E-PRLTAO-100-030808 for numerical estimates. For more information on EPAPS, see http://www.aip.org/pubservs/epaps.html.

[24] W. Hagen, A. Tielens, and J. M. Greenberg, Chem. Phys. **56**, 367 (1981).

[25] T. M. Chang and L. X. Dang, Chem. Rev. **106**, 1305 (2006) and references therein.

[26] P. Jungwirth and D. J. Tobias, J. Phys. Chem. B **105**, 10468 (2001).

[27] P. Jungwirth and D. J. Tobias, J. Phys. Chem. B **106**, 6361 (2002).